

Seasonal Cap Cover and Compositional Variability as observed by MARCI, CTX, and CRISM for MY28-MY31. Calvin¹, W. M. James², P.B., Thomas³, P.C. and Dixon¹, E.M. ¹Geological Sci., MS 172, University of Nevada, Reno, NV 89557 (wcalvin@unr.edu). ²Space Science Institute, 4750 Walnut Street, #205, Boulder, CO. ³Center for Radiophysics and Space Research, Cornell University, Ithaca NY 14853.

Introduction: Observations using the Mars Reconnaissance Orbiter (MRO) instruments have occurred over three martian years (MY) 28, 29, and 30, with MY31 just beginning. We have observed the seasonal cap recessions in both the north and south using MARCI daily global images and have examined the composition of selected units of the polar layered deposits using CRISM. CTX allows us to relate the composition to surface geomorphology of the deposits. Observations over multiple Mars years allows us to compare changes between years, begin a detailed examination of exposed volatile ices and their variability, as well as explore longer term evolution of the high albedo deposits at the poles.

Observations: Mars Reconnaissance Orbiter has been in mapping orbit since fall of 2006, Ls ~ 120 of MY 28. Note the MY nomenclature follows that identified by [1]. Table 1 summarizes the Earth dates and Mars Years for seasonal cap retreat and summer observations of the polar region. To date we have observed 3 seasonal recession periods for both the north and the south, and two full summer seasons for the residual ice deposits both north and south as well.

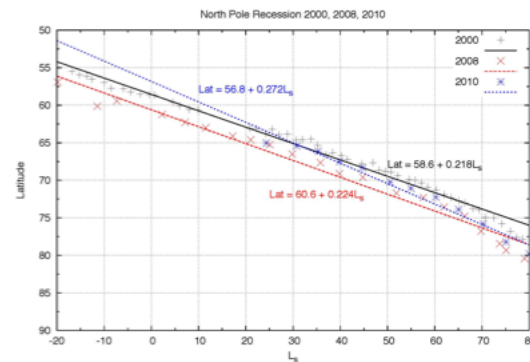
Table 1: MRO Observations by Earth date and Ls

Mars Year Earth Date of Ls=0	North Recession Ls 25 to 95	North Summer Ls 90 to 180	South Recession Ls 180 to 330	South Summer Ls 320 to 360
MY 28 1/21/2006	Not observed, before Sci Ops	Start ~Ls 120 11/06 – 1/07	4/07 -9/07 Planet wide dust event	10/07 – 12/07
MY 29 12/9/2007	2/08 – 7/08	7/08 – 12/08	12/08 to 8/09	Not observed (spacecraft recovery)
MY 30 10/26/2009	12/09 – 5/10	5/10 – 11/10	11/10 to 7/11	7/11 to 9/11
MY 31 9/13/2011	Not processed yet!	Being Collected (Ls 111)		

North Seasonal Cap Recession: Spacecraft observations of the northern cap recession have been made using MOC, TES, OMEGA, MARCI, and CRISM [e.g. 2-6]. Calvin et al. [5] presented seasonal cap recession movies as observed in both MY 29 and 30. Recession patterns observed in MY 30 are similar to those described for MY 29 [7]. Significant variability in the early season is noted in both years and the retreating seasonal cap edge is extremely

dynamic. In particular, large scale “defrosting” or loss of high albedo material is observed up to approximately Ls 95. Ls of the minimum in high albedo coverage is the same between the two years. However, details of the high albedo deposit cover are variable. In both MY 29 and 30, the Gemini Scopuli troughs darken up to ~Ls 100 and then brighten. We note that the extent of high albedo deposits after Ls 100 is greater in MY29 and the area identified as gypsum [e.g. 8] is also covered longer by high albedo frost. Both years have large dust storms at ~ Ls 155 (onset of polar hood formation) but the source of dust appears different in each Mars year. Dust appears to arrive from lower latitudes in MY29, but emerges from Chasma Boreale in MY30. It should be noted that the MY 29 summer followed the large planet encircling storm of 2007 – perhaps cooler overall temperatures lead to more extensive cover? Dixon et al. [9] compared the seasonal cap recession curves for MY 25, 28 and 29 (2000, 2008, 2010) and found them to be similar, with MY 28 retreating to higher latitudes at an earlier Ls, as shown in Figure 1. In general, linear fits are modest, but not perfect and all three years exhibit a change in recession rate from Ls ~ 25 to 65. It is interesting to note that this corresponds with the time when the surface cover appears to shift to the signature of water frost even though CO₂ ice is still present [4].

Figure 1: Average latitude of north seasonal cap recession.

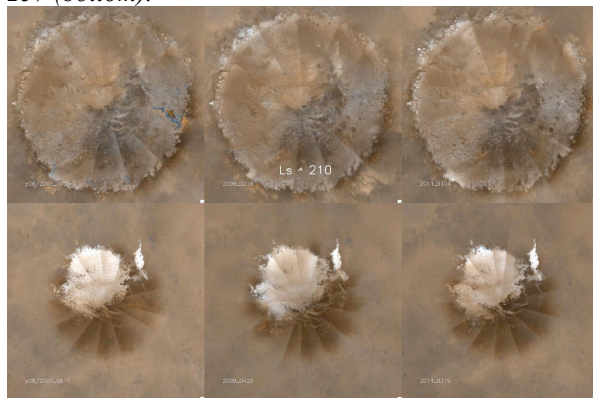


South Seasonal Cap Recession: Spacecraft observations of the southern seasonal cap recession have been made using MOC, TES, OMEGA and CRISM [e.g. 10-13]. The asymmetric retreat of the seasonal cap has been known from many previous

observations, but although the “Mountains of Mitchel” were known in the 19th century, the MOC observations by James et al. [10] are the first to image the seasonal retreat for all longitudes in a polar stereo projection with comprehensive seasonal coverage from Ls 170 to 280. Kieffer et al. [11] coined the term “cryptic region” for an area within the retreating seasonal cap that develops a very low albedo, but retains the cold temperature of CO₂ ice in equilibrium with the atmospheric temperature. This dark region is also clearly seen in the retreat in MOC [10]. The visual appearance of retreating seasonal frost is largely symmetric around the pole until ~ Ls 220 when the edge of the bright seasonal frost encroaches on the cryptic region and retreat appears to become asymmetric and more centralized on the south residual polar ice dome. Kieffer et al. [11] also note that the optical and thermal “crocus maps” (edge of last CO₂ frost as determined by visual appearance or temperature) are dissimilar between Ls 225 and 245.

Calvin et al. presented south cap retreat images for MY 28, 29 and 30 from MARCI at both the 5th International Polar Conference [5] and at this meeting. The daily global map product used for these early assessments imparts longitudinal averaging at a fixed latitude in order to smooth out seams between the different MARCI frames. This leaves a dark image artifact for latitudes in the lower right quadrant of the frames that is due to retention of high albedo material at lower latitudes in the upper left quadrant. Figure 2 shows a snapshot for the three Mars years near Ls 210 and 257. The latter is roughly when the optical and thermal maps of CO₂ extent are again similar [11].

Figure 2: South cap recession for MY 28 (left), 29 (center) and 30 (right) from MARCI. Ls 210 (top) and 257 (bottom).



Full analysis of cap recession and comparison with previous observations will require calibration and mosaicking that preserves the true surface albedo for

all of the MARCI filters. This work is presently underway. What can be inferred even through these preliminary mosaics are that the retreat in MY28 is more rapid, coinciding with the large planet-encircling dust storm that year. The onset of dust across the polar region is obvious at Ls 265. There appear to be annual differences in deposit thickness extent and appearance of the cryptic region and timing of retreats in each of the three Mars years. There is a persistent late bright outlier that correlates with observations of remnant water ice at the base of the SPLD residual ice dome [12, 14] and this outlier disappears in MY28, but is preserved in MY 29 and 30.

Initial CRISM Observations North Residual Ice:

Calvin et al. [8] summarized a number of CRISM observations from MY 28 (late northern summer). They found hydrated materials occur throughout the north polar layered deposit (NPLD) and in windows exposing the lower stratigraphy. Gypsum appeared on the dune crests, not troughs or inter-dune areas. In general, the PLD is water ice rich, including the “dark” layers and lanes. This is consistent with radar observations that infer largely clean ice in order to get large scale propagation of radar waves through the NPLD [15]. Band depth mapping was performed on several images to show that ice band strength can provide an unique marker of stratigraphy and is independent of albedo. The lowest units are also ice rich and ice lenses link upper and lower compositional units, perhaps related to slumping, avalanches or other mass wasting processes.

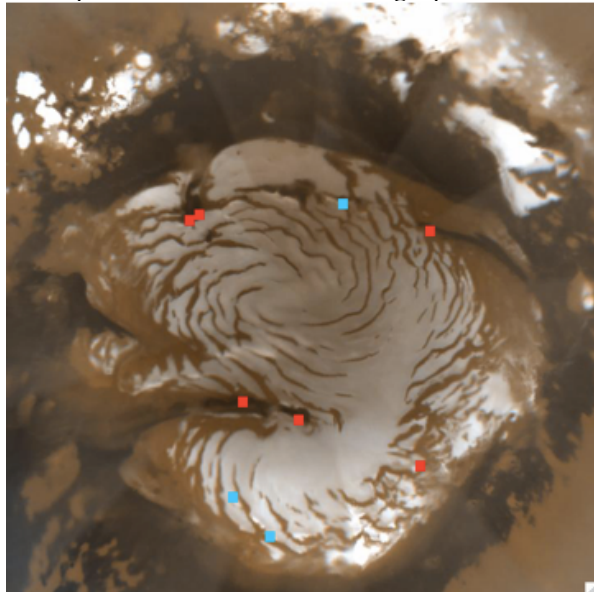
North Residual Ice Seasonal Change: With multiple mars years of observations, several sites have been subject to repeated observation by CRISM, CTX and HiRISE to observe behavior both during the seasonal recession as well as summer evolution.

Evolution of Bright Patches. Calvin and Titus [16] noted several regions where high albedo material persisted throughout the northern summer in TES seasonal mosaics. Several of these spots were identified for monitoring and Cantor et al. [7] presented analysis of one selected bright patch, which disappeared in MY 28. These spots occur on the margins of the high albedo material, on the flat slopes above steep scarps. Monitoring of one location with CRISM full resolution data shows variation in water ice band depth over the summer season, even in data acquired through light atmospheric dust hazes, which inverts the typical visual albedo, making ice surfaces darker and dark lanes brighter. We are currently exploring the use of ice band depth as a monitor of the evolution of these spots, regardless of atmospheric

conditions, but this work requires more detailed study of additional spots.

Seasonal Frosts at High Resolution. Appéré et al. [4] have noted the transition in the retreating north seasonal cap from the surface signature dominated by the spectral features of CO₂ ice to those of H₂O ice near Ls 25. They have postulated development of a thin water ice coating over the retreating CO₂ seasonal deposit. Six sites have been subject to detailed retreat monitoring with CRISM and HiRISE (Figure 3), allowing us to explore the distribution of these two ices at higher spatial resolution.

Figure 3: Locations for monitoring with CRISM and HiRISE. Red squares are seasonal retreat monitoring. Blue squares are summer season bright patches.



Preliminary analysis of two of these sites shows a transition from carbon dioxide to water spectral shapes, however subtle spectral slopes suggest that CO₂ ice is never “absent” and that later season spectral shapes are mixed, while dominated by the water ice component. Scenes at each Ls also show variation of carbon dioxide band strength within the scene and cold trapping of carbon dioxide on scarp walls and on trough floors over ice-cemented layers. Defrosting dunes show stronger CO₂ signatures, suggesting jet like defrosting and recondensation of CO₂ near the jets, similar to that observed in the south and also proposed for the north based on HiRISE images [17,18].

Initial CRISM Observations South Residual Ice:

Full resolution targetted CRISM observations (FRTs) were first explored to see if there were compositional differences associated with various pits, mesas and

linear features of the south residual CO₂ ice cap. This upper surface is shown to be undergoing a complex pattern of erosion and deposition, based on MOC and CTX images [e.g. 19, 20]. Thomas et al. [20] found however that there did not appear to be any compositional link to erosion of mesas. These were found to have variable and small amounts of water ice. Additionally they noted, CO₂ ice signatures are ubiquitous until as late as Ls 320 [also 21]. Strong CO₂ ice features at 2.28 and 2.34 μm appear in dark terrain both early and late in the summer suggesting large pathlengths in ice and that the dark lanes may be CO₂ ice cemented soils. Thomas et al. [20] also noted a transition zone between the high albedo residual cap to the dark “PLD” underneath that has more water. This suggests there may be an underlying layer where water becomes the dominant composition, but more observations over a wider area need to be examined to verify this. Unlike the northern PLD, areas of dark lanes without any water ice signature were noted. Water ice was also observed as a “patina” or cold trapped on shadowed slopes. In this preliminary survey water ice was never more than a few wt % based on previous mixture modeling.

References:

- [1] Clancy, T. et al. J. Geophys. Res. 105 (E4), 9553–9572, 2000.
- [2] James, P. B. and B. A. Cantor, Icarus, 154, p. 131, 2001.
- [3] Kieffer, H. H. and T. N. Titus, Icarus, 154, p. 162, 2001.
- [4] Appéré, T. et al. JGR 116, doi:10.1029/2010JE003762, 2011.
- [5] Calvin, W. M. et al. 5th Mars Polar Conf #6077.
- [6] Brown, A.J. 5th Mars Polar Conf. #6060.
- [7] Cantor, B. A. et al. Icarus, 208 (1), pp. 61-81, 2010.
- [8] Calvin, W. M. et al. J. Geophys. Res. 114, E00D11, doi:10.1029/2009JE003348, 2009.
- [9] Dixon, E. M. et al. 43rd LPSC, Abstract #2798, 2012.
- [10] James, P.B. et al. J. Geophys. Res., vol. 106, E10, 23635-23652, 2001.
- [11] Kieffer, H. H. et al., J. Geophys. Res., vol. 105, E4, 9653-9699, 2000.
- [12] Langevin, Y. et al., J. Geophys. Res. 112, E08S12, doi:10.1029/2006JE002841, 2007.
- [13] Brown, A.J. et al., J. Geophys. Res., 115, E00D13, doi:10.1029/2009JE003333, 2010.
- [14] Piqueux, S. J. Geophys. Res. 113, E08014, doi:10.1029/2007JE003055, 2008.
- [15] Phillips, R.J. et al. Science, 320, 1182, doi:10.1126/science.1157546, 2008.
- [16] Calvin, W. M. and T. N. Titus, Planet. Space Sci., 56, p. 212, 2008.
- [17] Kieffer, H. H. et al., Nature, Vol 442, p. 793, doi:10.1038/nature04945, 2006.
- [18] Hansen, C. J. et al., Science, 331, p.575, DOI: 10.1126/science.1197636, 2011.
- [19] Thomas, P. C. et al., Icarus, 174, 535-559, 2005.
- [20] Thomas, P. C., et al., Icarus, 203, 352-375, 2009.
- [21] Calvin, W. M. 40th LPSC, #1984, 2009.